Dissociation of N_2 on chromium alloys: A general mechanism for dissociation of diatomic molecules

T. C. Guimarães* and A. C. Pavão
Departamento de Quimica Fundamental, Universidade Federal de Pernambuco, Cidade Universitaria, CEP 50670/901, Recife PE, Brazil

C. A. Taft
Departamento de Materia Condensada e Física Estatistica, Centro Brasileiro de Pesquisas Físicas, Rua Dr. Xavier Sigaud, 150, CEP 22290-180, Rio de Janeiro, Brazil

W. A. Lester, Jr.
Chemical Sciences Division, Lawrence Berkeley National Laboratory and Department of Chemistry, University of California, Berkeley, California 94720-1460

(Received 28 August 1998)

In this work we use *ab initio* Hartree-Fock effective core potentials to analyze N_2 dissociation on doped (bimetallic) Cr (110) surfaces described by Cr_4MN_2 and $Cr_3M_2N_2$ (M = Sc, Ti, V, Fe, Co, Ni, Zn, Mg, Ca) clusters in both perpendicular and inclined configurations. Our results indicate that the inclined state is energetically more favorable than the perpendicular configuration. In comparison with monometallic surfaces, some of the bimetallic systems, such as Cr_4ScN_2, Cr_4TiN_2, and $Cr_3V_2N_2$, are found to have larger N-N distances, surface→N_2 charge transfers, higher Fermi energies, and smaller N-N stretching frequencies, indicating greater efficiency of these alloys for dissociation. The theoretical parameters obtained from these bimetallic catalytic systems are interpreted using a general mechanism proposed for dissociation of diatomic molecules on transition metal surfaces. [S0163-1829(99)02639-9]

I. INTRODUCTION

The efficiency of transition-metal alloys for N_2 dissociation is of considerable theoretical, experimental, and technological interest. The N_2 dissociative reactions are important in heterogeneous catalytic processes[1–36] for the synthesis of ammonia, the stability of ceramic-metal interfaces, as well as the preparation of nitride layers. A comparison of isoelectronic CO chemisorption and dissociation with that of N_2 may provide useful information on how the latter interacts with metallic and alloy surfaces (Fig. 1). In the linear metal-CO complex, the interaction is described by the Blyholder model in which a bond is formed by the electron transfer from a $5s$ orbital of CO to unoccupied metal orbitals accompanied by the back donation of electrons from occupied d orbitals into unoccupied $2\pi^*$ orbitals of CO. A similar picture can be used to describe the bonding of a metal-N_2 complex for which the molecular orbitals that participate predominantly in bonding to the surface are the donating orbitals $3\sigma_g$ and $2\sigma_u$ which are essentially nonbonding. In CO the $2\pi^*$ orbital is localized mainly on carbon so that adsorption occurs via metal-carbon bonding whereas N_2 is adsorbed via a metal-nitrogen bond. On most densely packed metal surfaces CO is adsorbed with the molecular axis parallel to the surface normal whereas on some surfaces, such as Fe (100) and Cr (110), a tilted CO molecular state is also observed. Although N_2 generally chemisorbs with its intramolecular axis approximately perpendicular to the transition-metal surface,[9–15] some experiments[16–19] have indicated that N_2 is strongly chemisorbed on Cr (110) and other surfaces with its bond axis parallel to the surface, which is not explained by the Blyholder model. We have previously used a mechanism based on Pauling's theory of nonsynchronized resonance of valence bonds[5–8,20,28] in order to analyze the catalytic process of N_2 dissociation on a Cr (110) surface.[8] This model will also be used in this work to analyze the dissociation of N_2 on model alloys.

Research efforts focusing on coadsorption of CO with alkaline metals on the surface of transition metals have suggested various mechanisms[21–36] to explain the observed decrease in vibrational frequency and increase of catalytic activity of the dissociated CO. Many of these mechanisms are based on some type of induced enhanced back bonding, i.e., modifications of Blyholder's model in which alkali-

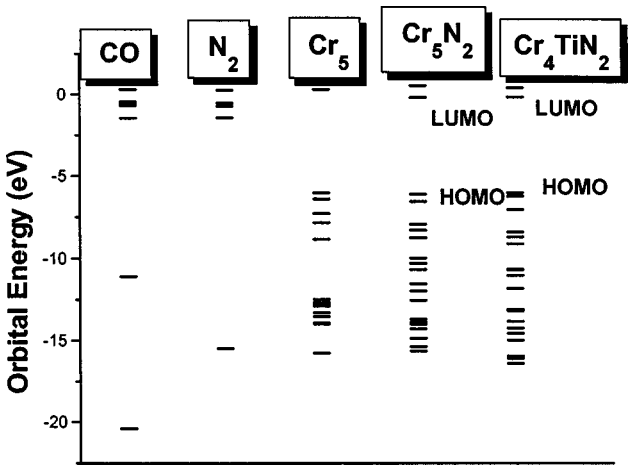

FIG. 1. Model for catalytic dissociation of diatomic molecules on transition-metal or model alloy surfaces.

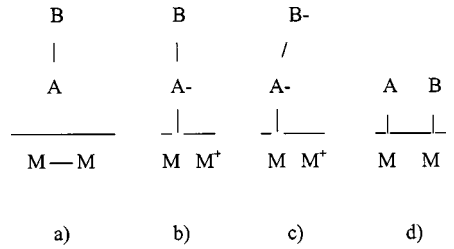

FIG. 2. Orbital self-consistent-field energies for CO, N_2, the bare cluster Cr_5, as well as the inclined Cr_5N_2 and Cr_4TiN_2 configurations.

metal atoms can also cause increased charge transfer to CO $2\pi^*$ orbitals. This weakens the CO bond, decreases the vibrational frequency, and increases catalytic activity. Our proposed model for N_2 dissociation on chromium alloys, without coadsorption, also uses a modification of the Blyholder model in which induced enhanced back-bonding electron transfer to N_2 antibonding orbitals can be attributed to effects to be described, including the inclination of N_2 and doping of the metals. Our work shows how orbital energies are modified as a result of inclination and doping. We use *ab initio* Hartree-Fock calculations to study the N_2 interaction with doped Cr (110) surfaces described by Cr_4MN_2 and $Cr_3M_2N_2$ (M = Sc, Ti, V, Fe, CO, Ni, Zn, Mg, Ca) clusters in both perpendicular and inclined configurations. We determine optimized geometries, charge transfers, Fermi energies, and stretching frequencies. A general mechanism is proposed for dissociation of diatomic molecules on metallic and bimetallic surfaces based on the theory of nonsynchronized resonance of covalent bonds.[5–8,28]

II. COMPUTATIONAL DETAILS

The calculations were carried out using Gaussian 92 (Ref. 37) in the Hartree-Fock method with effective core potentials and the Hay and Wadt basis set.[38] As in our previous work,[8] we focus on Cr (110) in which tilted N_2 configurations have been observed. One or two metallic atoms of the Cr_5 cluster in the Cr (110) plane were substituted by Sc, Ti, V, Fe, Co, Ni, Zn, Mg, and Ca whereas the N_2 geometry was fully optimized yielding relaxed interatomic distances and angles. Despite the often serious limitations to cluster quantum chemical methods, in our previous work[5–8,28] we have shown that, in agreement with other workers using smaller clusters for transition-metal surfaces with adsorbed diatomic molecules in a comparative analysis among various geometries, that the calculated charge transfer is in reasonable agreement with experiment. We did not simulate doping by charging the cluster in an attempt to better describe the local interaction between the dopant M and N_2. We have kept the crystal atoms fixed at the isolated crystal geometry during the calculations. Coulbourn and Mackrodt[9(d)] investigated relaxation effects in oxides and found regarding cation impurities, after considering a wide range of possibilities including size and charge states, no major differences in adsorption characteristics from those of the planar undoped surface. Our previous work using larger clusters with transition-metal dopants in metal oxides indicated that freezing the positions of the crystal atoms in the calculations did not appear to affect our results and main conclusions.[9(a)–9(c)]

TABLE I. Optimized gemoetry for the Cr_4TiN_2 cluster representation of the Cr (110) surface.

Geometries[a]	d(N-N)[d]	d(surf-N)[e]	d(Cri-PrN)[f]	α[g]	β[h]
Inclined[b]	1.474	1.020	1.530	11.31	53.93
Perpendicular[c]	1.364	1.084		90.0	0.0

[a]Optimized geometry with fixed Cr-Cr experimental interatomic distances.
[b]N_2 inclined towards surface.
[c]N_2 perpendicular to surface.
[d]d(N-N) indicate interatomic distances (Å) between N1 and N2.
[e]d(surf-N) indicates the perpendicular height (Å) of N1, first nitrogen, above the surface.
[f]d[Cri-Pr(N)], i=1,2, indicates the distance (Å) between Cri (i=1) and the projection of N on the Cr1-Cr2 axis.
[g]α indicates the angle (degrees) between the N_2 bond axis and the surface.
[h]β indicates the rotation angle (degrees) of nearly parallel N_2 bond axis from short axis towards long-axis direction.

TABLE II. Total energies, Fermi energies, HOMO-LUMO, surface→N_2 charge transfers, stretching frequencies for the Cr_4TiN_2 cluster representation of the Cr (110) surface.

Geometries[a]	E_{Total}[b] (1×10^3)	E_F[c]	ΔE[d]	Charge transfer[e]	N_2 stretch frequency[f]
Inclined	−4.755	−6.009	−5.858	−0.79	1052
Perpendicular	−4.071	−5.683	−5.620	−0.53	1303

[a]Optimized geometries described in Table I.
[b]E_{total} denotes total energy (eV).
[c]E_F denotes Fermi energy (eV).
[d]ΔE denotes HOMO-LUMO energy difference (eV).
[e]Mulliken surface→N_2 charge transfer (a.u.).
[f]Stretching frequency (cm^{-1}).

III. MODEL

The model proposed for the dissociation of diatomic molecules on pure and bimetallic transition-metal surfaces consists of a process of electron transfer from $M \rightarrow X_2$ and $X_2 \rightarrow M$ (where M is a metal and X_2 is a diatomic molecule) via molecular states. This mechanism is based on the theory of nonsynchronized resonance of covalent bonds introduced by

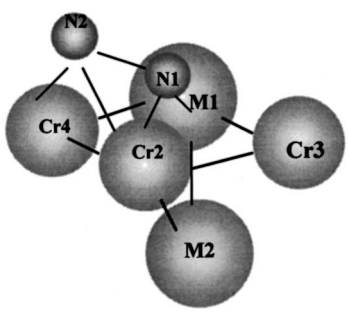

FIG. 3. Interaction of N_2 on the Cr_4MN_2 and $Cr_3M_2N_2$ model representations of the Cr (110) surface (we use $M1$ for Cr_4MN_2 and $M1$ and $M2$ for $Cr_3M_2N_2$ clusters).

TABLE III. Optimized geometries for the inclined configurations for the systems Cr_4N_2, ScN_2, Cr_4TiN_2, $Cr_3V_2N_2$, Cr_4FeN_2, $Cr_3Fe_2N_2$, $Cr_3Co_2N_2$, Cr_4NiN_2, and Cr_4ZnN_2 describing the Cr (110) surface.

Systems	Charge of N2[a]	d(N-N)[b]	d(surf-N)[c]	d(Cri-PrN)[d]	α[e]	β[f]
Cr_5N_2	−0.306	1.428	0.996	1.482	14.18	59.08
Cr_4ScN_2	−0.242	1.466	0.997	1.450	15.97	60.09
Cr_4TiN_2	−0.306	1.474	1.020	1.474	11.31	53.93
$Cr_3V_2N_2$	−0.205	1.462	0.995	1.482	15.13	59.08
Cr_4FeN_2	−0.297	1.428	0.995	1.443	13.88	60.62
$Cr_3Fe_2N_2$	−0.308	1.438	0.983	1.482	14.10	57.68
$Cr_3Co_2N_2$	−0.296	1.428	0.994	1.442	13.80	60.61
Cr_4NiN_2	−0.298	1.424	0.965	1.493	14.90	58.80
Cr_4ZnN_2	−0.311	1.424	0.973	1.453	15.56	60.71

[a]Mulliken charge (a.u.) on N2, the nitrogen atom furthest from the surface.
[b]d(N-N) indicate interatomic distances (Å) between N1 and N2.
[c]d(surf-N) indicates, perpendicular height of N1, first nitrogen, above the surface.
[d]d(Cri-PrN), $i=1,2$, indicates the distance between Cri ($i=1$) and the projection of N on the Cr1-Cr2 axis.
[e]α indicates the angle (degrees) between the N_2 bond axis and the surface.
[f]β indicates the rotation angle (degrees) of the nearly parallel N_2 bond axis from the short-axis towards long-axis direction.

Pauling[20,5–8] to explain the movement of negative charges in a metal as a resonance of covalent bonds from one position to another, via successive changes of simple bonds. Figures 2(a) and 2(b) describe the resonance components of the N_2 dissociation process and the latter two panels [2(c) and 2(d)] describe the dissociation processs induced by this resonance.

The first stage of the model [Fig. 2(a)] shows molecule *AB* at the *M-M* surface; here *M* denotes a transition-metal atom). Figure 2(b) depicts the transfer of an electron from the surface to the diatomic molecule, followed in Fig. 2(c) with the redistribution of charge into an antibonding orbital. In the catalytic process, however, the transferred electron must return to the surface in order to restore the electroneutrality of the catalyst. In the last stage, Fig. 2(d), the *A-B* bond is broken with resultant bonding of *A* and *B* to the metal. Inclination has resulted in a configuration more favorable for the formation of bonds to the surface due to the gradual increase of the negative charge on atom *B*, making it attracted more to substrate atoms that possess a formal positive charge. The electron returns to the surface, restoring the electroneutrality of the catalyst, while the *A-B* bond is broken.

IV. RESULTS AND DISCUSSIONS

We begin with transition metals, afterwards we will discuss alkaline metals. In Table I we give the optimized geometries of the Cr_4TiN_2 cluster description of the Cr (110) surface. In Table II we list total energies, Fermi energies [highest occupied molecular orbital (HOMO)], HOMO-LUMO (lowest unoccupied molecular orbital) energy differences, charge transfers, and stretching frequencies. In Fig. 1 we show the orbital energies for CO, N_2, the bare cluster, the inclined Cr_5N_2, and the Cr_5TiN_2 cluster configurations (Fig. 3) which reflect changes in positions, densities, and Fermi levels with inclination and doping. In agreement with our previous work,[8] the present results indicate that the predissociative inclined state of Cr_5TiN_2 is more favorable for dissociation than the perpendicular configuration. In the inclined configuration, the N-N distance increases, the surface→N_2 and N1→N2 (nitrogen atoms closer and further from the surface, respectively) charge transfers increase, the Fermi energy goes to higher levels and the N-N stretching frequency diminishes. Similar effects were also observed for the other bimetallic systems investigated, namely, Cr_4ScN_2, $Cr_3V_2N_2$, Cr_4FeN_2, $Cr_3Fe_2N_2$, $Cr_3CO_2N_2$, Cr_4NiN_2, and Cr_4ZnN_2 (Fig. 3).

In Tables III and IV we give optimized geometries for inclined Cr_5N_2, Cr_4ScN_2, Cr_4TiN_2, $Cr_3V_2N_2$, Cr_4FeN_2, $Cr_3Fe_2N_2$, $Cr_3Co_2N_2$, Cr_4NiN_2, and Cr_4ZnN_2 configurations describing the Cr (110) surface as well as the HOMO-

TABLE IV. HOMO-LUMO, Fermi energies, surface N_2 charge transfers, stretching frequencies of the most stable inclined configurations for the Cr_5N_2, Cr_4ScN_2, Cr_4TiN_2, $Cr_3V_2N_2$, Cr_4FeN_2, $Cr_3Fe_2N_2$, $Cr_3Co_2N_2$, Cr_4NiN_2, and Cr_4ZnN_2 clusters describing the Cr (110) surface.

System[a]	ΔE[b] (eV)	E_F[c] (eV)	Charge transfer[d]	N_2 stretching frequency (cm^{-1})
Cr_5N_2	−5.93	−6.114	−0.79	1220
Cr_4ScN_2	−5.59	−5.755	−0.74	1100
Cr_4TiN_2	−5.86	−6.009	−0.79	1052
$Cr_3V_2N_2$	−6.04	−6.063	−0.69	1110
Cr_4FeN_2	−6.00	−6.219	−0.77	1250
$Cr_3Fe_2N_2$	−5.83	−6.042	−0.79	1241
$Cr_4Co_2N_2$	−6.00	−6.220	−0.77	1251
Cr_4NiN_2	−5.78	−6.004	−0.74	1245
Cr_4ZnN_2	−5.74	−5.739	−0.80	1246

[a]Optimized geometries as described in Table I.
[b]ΔE (eV) denotes the HOMO-LUMO energy difference.
[c]E_F denotes Fermi energy (eV).
[d]Mulliken surface→N_2. Charge transfer (a.u.).
[e]N-N stretching frequency (cm^{-1}).

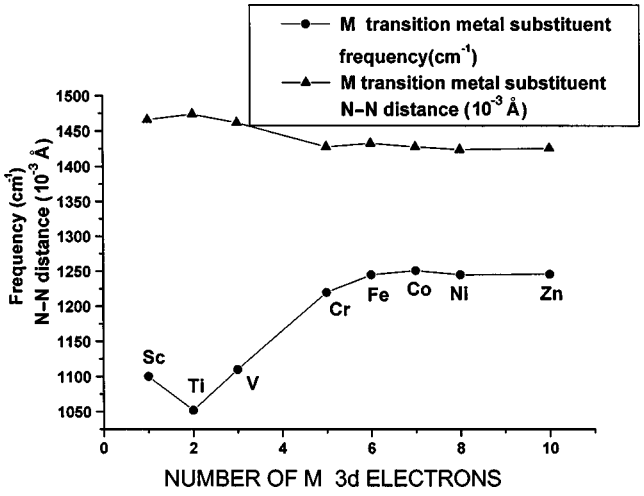

FIG. 4. Stretching frequency (cm^{-1}) and N-N distance (Å) for Cr_4MN_2, $Cr_3M_2N_2$ (average values used for $Cr_3Fe_2N_2$ and Cr_4FeN_2) vs the number of $3d$ electrons of M (Sc, Ti, V, Cr, Fe, Co, Ni, and Zn).

LUMO energy differences, Fermi energies, surface$\rightarrow N_2$ charge transfer, and N-N stretching frequencies. Results for the pure Cr_5N_2 system[8] are also given for comparison. We note that in relation to the pure Cr_5N_2 system, Cr_4ScN_2, Cr_4TiN_2, and $Cr_3V_2N_2$, show larger N-N distances (Table III), high Fermi energies, large surface$\rightarrow N_2$ charge transfer (Table IV) and smaller N-N stretching frequencies, indicating greater efficiency of these systems for the dissociation process. We note that the largest N-N distance (1.474 Å), the smallest stretching frequency (1052 cm^{-1}) as well as a large charge transfer is found for $CrTiN_2$. Our results from Tables III and IV suggest that the most efficient alloy for dissociation of N_2 should be Cr_4TiN_2. A comparison of Cr_4FeN_2 with $Cr_3Fe_2N_2$ (Tables III and IV) shows that an increase in the dopant concentration increases the surface$\rightarrow N_2$ charge transfer and the N-N distance, leading to more efficient dissociation. These tables also show smaller N_2 stretching frequencies and large N-N distances for doping with elements to the left of the Periodic Table whereas there are no significant differences for Fe, Co, Ni, and Zn (Fig. 4). These findings suggest that the more efficient surfaces are those doped with atoms having low $3d$ occupation.

Geometrical effects may be important in dissociation of diatomic molecules on bimetallic systems. We note that the differences between the atomic radii of Sc, Ti, and V and the atomic radius of Cr are 0.36, 0.20, and 0.07 Å, respectively, whereas the atomic radii of Cr, Mn, Fe, Co, and Ni are similar. Zn constitutes an exception to the rule owing to its $[Ar]3d^{10}4s^2$ configuration in which all orbitals are filled. This suggests that a geometric effect based on the atomic radius of the substituent transition metal may also play a role in the catalytic process. Surface irregularities caused by the substitution of metals may alter the potential and orbital overlaps to which N_2 is subjected when interacting with a surface leading to enhanced conditions for dissociation.

Our results in Table IV suggest that doping with transition metals can reduce the HOMO-LUMO energy difference, raise the Fermi level and, consequently, increase the capacity of the metal for back donation. Doping can also lead to the formation of irregularities on the surface due to differences in atomic radius and modification of the number of available electrons and holes for charge transfer. These effects favor an inclined predissociative state, which is a crucial phase in the cyclic process of electron transfer described by the present model; see Fig. 2.

We now turn to alkaline metals. In Tables V and VI we present optimized geometries, HOMO-LUMO energy differences, Fermi energies, charge transfers, and stretching frequencies for the $Cr_3Ca_2N_2$, Cr_4CaN_2, and Cr_4MgN_2 systems in their most stable inclined configurations. In Table VII we list Mulliken atomic charge distributions for the $Cr_3Ca_2N_2$, Cr_4CaN_2, $Cr_3Fe_2N_2$, Cr_4TiN_2, and Cr_4MgN_2 configurations. The donated electrons are delocalized and occupy an orbital with energy that depends on the cluster size and dopant atom; however, the present molecular-orbital calculations show that the electron is mainly localized on N_2, in agreement with the resonating valence bond description. We also note that for $Cr_3Ca_2N_2$, Cr_4CaN_2, and Cr_4MgN_2— although indicating larger surface$\rightarrow N_2$ charge transfers of 0.97, 0.92, and 0.81, respectively—the amount of charge transferred to the second nitrogen N2 is only 0.279, 0.286, and 0.290, respectively, i.e., it is smaller in magnitude than that transferred by the Cr_5N_2 (-0.306), Cr_5TiN_2 (-0.306), and

TABLE V. Optimized geometries for inclined configurations with Cr_5N_2, Cr_4CaN_2, $Cr_3Ca_2N_2$, and Cr_4MgN_2 describing the Cr (110) surface.

System	Charge of N2[a]	d(N-N)[b]	d(surf-N)[c]	d(Cri-PrN)[d]	α[e]	β[f]
Cr_5N_2	-0.306	1.428	0.996	1.482	14.18	59.08
$Cr_3Ca_2N_2$	-0.279	1.431	1.059	1.300	10.33	63.10
Cr_4CaN_2	-0.286	1.428	1.024	1.280	7.41	64.19
Cr_4MgN_2	-0.290	1.434	1.045	1.345	11.27	59.97

[a]Mulliken charge (a.u.) of the nitrogen atom furthest from the surface.
[b]d(N-N) indicate interatomic distances (Å) between N1 and N2.
[c]d(surf-N) indicates perpendicular height of N1, first nitrogen, above the surface.
[d]d(Cri-PrN), $i=1,2$, indicates the distance between Cri ($i=1$) and the projection of N on the Cr1-Cr2 axis.
[e]α indicates the angle (degrees) between the N_2 bond axis and the surface.
[f]β indicates the rotation angle (degrees) of the nearly parallel N_2 bond axis from the short axis towards long-axis direction.

TABLE VI. HOMO-LUMO, Fermi energies, surface→N_2 charge transfer, stretching frequencies for the most stable inclined configurations of the Cr_5N_2, $Cr_3Ca_2N_2$, Cr_4CaN_2, Cr_4MgN_2 clusters describing the Cr (110) surface.

System[a]	ΔE[b] (eV)	E_F[c] (eV)	Charge transfer[d]	N_2 stretching frequency[e] (cm^{-1})
Cr_5N_2	−5.93	−6.11	−0.79	1220
$Cr_3Ca_2N_2$	−5.16	−5.86	−0.97	1236
Cr_4CaN_2	−5.51	−5.99	−0.92	1234
Cr_4MgN_2	−5.65	−6.00	−0.81	1208

[a]Optimized geometries as described in Table I.
[b]ΔE denotes the HOMO-LUMO energy difference (eV).
[c]E_F denotes Fermi energy (eV).
[d]Charge-transfer (a.u.) surface→N_2.
[e]N_2 stretching frequency.

$Cr_3Fe_2N_2$ (−0.308) systems. Although the addition of Ca and Mg atoms to the crystalline lattice increases surface→N_2 charge transfer, it does not, based on our model, favor nonsynchronized covalent bond resonances, due perhaps to the difficulty of the electron to move from the first nitrogen (N1) to the second nitrogen (N2) and then from N2 to the surface. In the $Cr_3Ca_2N_2$, Cr_4CaN_2, and Cr_4MgN_2 systems, the surface→N1 charge transfer appears to be more efficient than N1→N2 transfer. The substitution of Cr for Ca and Mg could, in principle, reduce the *d* orbitals available for receiving transferred electrons when they return to the surface.

We note that although alkaline metals can contribute significantly to the increase of the N-N distances, one must be careful with the excess negative charge on the surface because, according to the present model, dissociation is also related to the resistance to electron transfer during the catalytic cycle. An increase of back donation may represent a necessary condition, but alone it is not sufficient for the most efficient dissociation. We also observe from Table VII that the first outer layer of the surface remains positive for the $CrTiN_2$, Cr_4CaN_2, $Cr_3Fe_2N_2$, and Cr_4MgN_2 systems, which is not the case for the $Cr_3Ca_2N_2$ system. In accordance with the present model a positively charged surface would help attract the N2 atom to the surface. Hypothetically, catalysts like $Cr_3Ca_2N_2$ and Cr_2CaN_2 may be less efficient due to blocking of the catalytic cycle.

The largest surface→N_2 charge transfers and the smallest HOMO-LUMO energy differences are found in the $Cr_3Ca_2N_2$ and Cr_4CaN_2 systems. The most efficient alkaline metal introduced in the surface was Mg. We note the larger N1→N2 charge transfer for Cr_4MgN_2 relative to Cr_4CaN_2 and Cr_3CaN_2. Further, Mg also has a higher ionization potential than Ca and, if it transfers fewer electrons to the surface, we will have a more positive surface which should, in principle, facilitate a larger N2→surface charge transfer needed to complete the proposed catalytic cycle, although the surface→N_2 charge transfer is less than that for systems with substituted Ca. In addition to yielding better charge transfer as anticipated by our model than that obtained by substituting Ca, Cr_4MgN_2 also has longer N-N distances and smaller stretching frequencies. Despite the importance of back donation, other factors also have to be taken into account for better overall efficiency of the catalytic process.

V. CONCLUSIONS

The interaction of N_2 with bimetallic surfaces serves as a good model for the study of the adsorption and dissociation mechanism of diatomic molecules on promoted transition-metal surfaces. Chromium surfaces doped with 3*d* transition (or alkaline) metals can be more efficient for the dissociation of N_2 by raising the Fermi energy to higher levels and reducing the HOMO-LUMO energy differences increasing back donation, inclination, and consequently dissociation. The addition of other transition metals increases the number of *d* orbitals for back donation. Some 3*d* transition metals, for example, Ti on a Cr (110) surface, also increase the number of *d* unoccupied orbitals available for the reception of the electrons for formation of bonds to the surface. Our results indicate that the best alloy of chromium for dissociation of N_2 is Cr_4TiN_2. Geometric effects caused by substitution can result in modifications of potentials and overlaps between N_2 and the surface yielding important effects for dissociation of diatomic molecules on bimetallic systems. An appropriate electronic configuration for the charge-transfer cycle together with an intermediate difference of 0.20 Å between the atomic radius of the substituted metal and Cr seems to be ideal. The efficiency of dissociation is related, according to our model, with an electron transfer cycle. The increase of back donation represents one necessary, but not sufficient, condition for the optimization of a dissociation reaction. Although the largest back donations correspond to the Cr_4ZnN_2, $Cr_3Ca_2N_2$, and Cr_4CaN_2 clusters, these systems have smaller N-N distances and consequently larger vibrational frequencies.

In this study we show that for a number of bimetallic

TABLE VII. Mulliken atomic charges (a.u.) for the systems $Cr_3Ca_2N_2$, Cr_4CaN_2, $Cr_3Fe_2N_2$, and Cr_4TiN_2.

$Cr_3Ca_2N_2$		Cr_4CaN_2		Cr_4MgN_2		$Cr_3Fe_2N_2$		Cr_4TiN_2	
Atom	Charge	Atom	Charge	Atom	Charge	Atom	Charge	Atom	Charge
Ca	0.739	Ca	0.824	Mg	0.777	Cr	0.116	Ti	0.369
Cr	0.139	Cr	0.287	Cr	0.270	Cr	0.384	Cr	0.229
Cr	−0.106	Cr	0.046	Cr	0.017	Fe	0.116	Cr	0.147
Cr	−0.125	Cr	0.052	Cr	0.104	Cr	0.340	Cr	0.168
Ca	0.327	Cr	−0.294	Cr	−0.291	Fe	−0.240	Cr	−0.126
N1	−0.695	N1	−0.630	N1	−0.524	N1	−0.477	N1	−0.480
N2	−0.279	N2	−0.286	N2	−0.290	N2	−0.309	N2	−0.306

systems, the predissociative or inclined configurations are more stable. The calculations presented here support the present model proposed to explain the dissociation of N_2 on pure and doped (alloys, bimetallic) transition metals. We suggest that this model can also be applied to the dissociation of other diatomic molecules. The introduction of other transition metals to the lattice can introduce more electrons for donation and more unoccupied orbitals to receive the electron when it returns to the surface. An important intermediate state with large charge transfer, in which the molecule is inclined to the surface, was observed for all the systems investigated. The results reported support the existence of an inclined molecular state which can be identified as the precursor state of dissociation.

ACKNOWLEDGMENTS

T.C.G. and A.C.P. acknowledge financial assistance from CNPq (Brazil). C.A.T. received financial assistance from PRONEX/FINEP/CNPq (Brazil). W.A.L. was supported by the Director, Office of Science, Office of Basic Energy Sciences, Chemical Sciences Division of the U.S. Department of Energy under Contract No. DE-AC03-76SF00098.

*Permanent address: Universidade do Estado de Bahia, Dept. de Ciencias Exatas e da Terra, Estrada das Barreiras 1, Narandiba, Salvador, Bahia, Brazil.

[1] Y. Debauge, M. Abon, J. C. Bertoline, J. Massardier, and A. Rochefort, Appl. Surf. Sci. **90**, 15 (1995).
[2] M. Krawczyk, L. Zommer, B. Lesiak, and A. Jablonski, Surf. Interface Anal. **25**, 3356 (1997).
[3] T. Zambelli, J. Wintterlin, J. P. Trost, and J. Ertl, Science **273**, 1688 (1986).
[4] G. Blyholder, J. Phys. Chem. **68**, 2772 (1964).
[5] A. C. Pavão, M. M. Soto, W. A. Lester, Jr., S. K. Lie, B. L. Hammond, and C. A. Taft, Phys. Rev. B **50**, 1868 (1994); A. C. Pavão, M. Braga, C. A. Taft, B. L. Hammond, and W. A. Lester, Jr., *ibid.* **43**, 6962 (1991); A. C. Pavão, M. Braga, W. A. Lester, Jr., B. L. Hammond, and C. A. Taft, *ibid.* **44**, 1910 (1991).
[6] A. C. Pavão, B. L. Hammond, M. M. Soto, W. A. Lester, Jr., and C. A. Taft, Surf. Sci. **323**, 340 (1995).
[7] A. C. Pavão, C. A. Taft, T. C. Guimarães, and W. A. Lester, Jr., Trends Chem. Phys. **3**, 109 (1994) and references therein; A. C. Pavão, T. C. Guimarães, S. K. Lie, C. A. Taft, and W. A. Lester, Jr., THEOCHEM **458**, 99 (1999) and references therein.
[8] T. C. Guimarães, A. C. Pavão, C. A. Taft, and W. A. Lester, Jr., Phys. Rev. B **56**, 7001 (1997).
[9] (a) A. L. Almeida, J. B. L. Martins, C. A. Taft, E. Longo, and W. A. Lester, Jr., J. Chem. Phys. **109**, 3671 (1998), and references contained therein; (b) Int. J. Quantum Chem. **71**, 153 (1999); (c) B. L. Martins, E. Longo, and C. A. Taft, *ibid.* **70**, 368 (1998); (d) E. A. Coulbourn and W. C. Mackrodt, Surf. Sci. **143**, 391 (1984).
[10] K. Horn, J. Dinardo, W. Eberhard, and E. W. Plummer, Surf. Sci. **118**, 465 (1982); B. E. Nieuwenhuys, *ibid.* **105**, 505 (1981).
[11] P. S. Bagus, C. R. Brundle, K. Hermman, and D. Menzel, J. Cryst. Growth **20**, 253 (1980).
[12] D. Heskett, E. W. Plummer, D. R. A. Depaola, W. Eberhardt, F. M. Hoffmann, and H. R. Moser, Surf. Sci. **164**, 490 (1985).
[13] E. Umbach, Solid State Commun. **51**, 365 (1984).
[14] D. E. Ibbotson, T. Wittrig, and W. H. Weinber, Surf. Sci. **110**, 313 (1981).
[15] R. A. DePaola and F. M. Hoffmann, Chem. Phys. Lett. **128**, 343 (1986).
[16] H. J. Freund, B. Bastos, R. P. Messmer, M. Grunze, H. Kuhlenbeck, and M. Neumann, Surf. Sci. **185**, 187 (1987).
[17] Y. Fukuda and M. Nagossi, Surf. Sci. **203**, L651 (1988).
[18] D. Shinn, Phys. Rev. B **41**, 9771 (1990).
[19] M. Grunze, M. Golze, W. Hirschwald, H. J. Freund, H. Pulm, U. Seip, M. C. Tsai, G. Ertl, and J. Kuppers, Phys. Rev. Lett. **53**, 850 (1984).
[20] L. Pauling, J. Solid State Chem. **54**, 297 (1984).
[21] H. S. Luftman, Y. M. Sun, and J. M. White, Surf. Sci. **141**, 82 (1984).
[22] A. Gorling, L. Ackermann, J. Lauber, P. Knappe, and N. Rosch, Surf. Sci. **286**, 26 (1993).
[23] T. W. Eberhard, R. A. DePaola, E. W. Hoffmann, D. Heskett, I. Strathy, and H. R. Moser, Phys. Rev. Lett. **54**, 1856 (1985).
[24] J. J. Weimer, E. Umbach, and D. Menzel, Surf. Sci. **155**, 133 (1985); J. J. Weimer and E. Umbach, Phys. Rev. B **30**, 4863 (1984).
[25] J. Paul, Nature (London) **323**, 701 (1986).
[26] P. E. M. Siegbahn, Surf. Sci. **269**, 276 (1992).
[27] N. D. Lang, S. Holloway, and J. K. Norskov, Surf. Sci. **150**, 24 (1985); E. Wimmer, C. L. Flu, and A. J. Freeman, Phys. Rev. Lett. **55**, 2618 (1985).
[28] C. A. Taft, T. C. Guimarães, A. C. Pavão, and W. A. Lester, Jr., Int. Rev. Phys. Chem. **18**, 163 (1999), and references contained therein.
[29] C. M. Mate, C. T. Kao, and G. A. Somorjai, Surf. Sci. **206**, 145 (1988).
[30] N. Rosch, A. Gorling, P. Knappe, and J. Lauber, Vacuum **41**, 150 (1990).
[31] D. Heskett, K. Strathy, E. W. Plummer, and R. A. de Paola, Phys. Rev. B **32**, 6222 (1985).
[32] P. A. Schultz, J. Vac. Sci. Technol. A **8**, 2425 (1990).
[33] P. A. Schultz and R. P. Messmer, Surf. Sci. **209**, 229 (1989).
[34] P. A. Schultz, C. H. Patterson, and R. P. Messmer, J. Vac. Sci. Technol. A **5**, 1061 (1987).
[35] M. Scheffler, C. Droste, A. Fleszar, F. Maca, G. Wachutka, and G. Bartzel, Physica B **172**, 143 (1991).
[36] G. Pacchioni and P. S. Bagus, Chem. Phys. **177**, 373 (1993).
[37] M. J. Frisch, G. W. Trucks, M. Head-Gordon, P. M. W. Gill, M. W. Wong, J. B. Foresman, B. G. Johnson, H. B. Schlegel, M. A. Robb, E. S. Repllogle, R. Gomperts, J. L. Andres, K. Rachavachari, J. S. Binkley, C. Gonzalez, R. L. Martin, D. J. Fox, D. J. Defrees, J. Baker, J. J. P. Stewart, and J. A. Pople, GAUSSIAN 92 (Gaussian Inc., Pittsburgh, PA, 1992).
[38] J. Hay and W. R. Wadt, J. Chem. Phys. **82**, 270 (1985).